Proceeding of the 15th ME-NETT conference

Measurement of the Bucking Loads and Modes of Stiffened Composite Panels

Pairod Singhatanadgid
Mechanical Engineering Department, Faculty of Engineering,
Chulalongkorn University, Bangkok 10330, Thailand.
Tel : +66-(0)-2218-6595, Fax : +66-(0)-2252-2889, E-mail : Pairod.S@Chula.ac.th

Abstract

Buckling loads and modes of stiffened composite plates were experimentally determined and compared with the analytical predictions obtained using the Ritz method. In the analytical procedure, the beam function derived from the vibration problem of stepped beams was proposed as an approximate displacement function. The problem formulation ultimately leads to an eigenvalue problem, which is solved using standard procedures. The lowest eigenvalue and its corresponding eigenvector are the predicted buckling load and mode, respectively. The experimental buckling loads were fairly well predicted. The discrepancy between prediction and measurement in term of percentage error in prediction had an average value of +8.62%. Similarly, measured buckling modes were very well predicted by the Ritz method using the proposed beam function. The experiment results confirmed the change of mode from global buckling to local buckling or the change of number of mode when transverse tension was increased.

Introduction

An "advanced" composite material is a material system which consists of high strength and high modulus fibers embedded within a matrix material. Fibers in advanced composites include graphite, silicon carbide, aramid polymer and boron. Most of the loads applied to the composite structure are carried by fibers which are held together by the matrix. The matrix protects fibers from abrasion and transfers stresses from one fiber to the next. Because of their high strength-to-weight and stiffness-to-weight ratios, composite materials are extensively used in many applications in the aerospace, automotive, and marine industries. A main benefit of composite material is an ability to be tailored, which may not be obtained from conventional isotropic materials. Engineers can design the fiber orientations within the composite so that the desired mechanical properties are achieved.

In many applications, composites are manufactured in form of thin plate-like structures. Consequently, failure of laminated plates arises not only from excessive stresses but also from buckling. The stability behavior of stiffened composite plates is not completely understood although stiffened structures are widely used [1-2]. Common objectives in studies devoted to the behavior of stiffened plates are to determine pre- and post-buckling behaviors and/or the ultimate strength of the stiffened structures[3]. In this study, buckling behavior was predicted numerically using the Ritz method [4], using proposed beam functions as the displacement fields. The accuracy of the numerical prediction was verified with the experimental study.

The stiffened plate considered in this study is shown schematically in Fig 1. The plate is simply supported and may be biaxially loaded. The panel is loaded in the y-direction with a transverse tensile load (N_y). The transverse tension is known and remains constant. Buckling is initiated by a compressive load (N_x) applied to the panel in the x-direction.

Analytical Study

The approximate out-of-plane displacement functions are written as

$$w = \sum_{m=1}^{M}\sum_{n=1}^{N} A_{mn} X_m(x) Y_n(y) \tag{1}$$

where A_{mn} are undetermined coefficients. $X_m(x)$ and $Y_n(y)$ are continuous functions of x and y, respectively. $X_m(x)$ can be selected as $\sin\left(\frac{m\pi x}{a}\right)$ because the stiffeners are placed parallel to the x axis. There is no change of the stiffness along the x direction. On the other hand, function $Y_n(y)$ has to be selected such that the presence of a stiffener in the middle of the plate, i.e. the change of stiffness in the y direction, is accounted for.

The function $Y_n(y)$ used in this study was derived from the problem of transverse vibration of a stepped beam [5]. The beam is composed of three sections (see Fig 2). Section 1 and section 3 have the same thickness and represent the skin section of the stiffened plate. They are thinner than section 2 which represents the stiffener section. The general form of $Y_n(y)$ is

$$Y_n(y) = \begin{cases} C_1 \sin k_1 y + C_2 \cos k_1 y \\ +C_3 \sinh k_1 y + C_4 \cosh k_1 y \quad \text{for } 0 \le y \le l_1 \\ \\ C_5 \sin k_2 y + C_6 \cos k_2 y \\ +C_7 \sinh k_2 y + C_8 \cosh k_2 y \quad \text{for } l_1 \le y \le l_2 \\ \\ C_9 \sin k_3 y + C_{10} \cos k_3 y \\ +C_{11} \sinh k_3 y + C_{12} \cosh k_3 y \quad \text{for } l_2 \le y \le l_3 \end{cases} \tag{2}$$

C_i and k_i are constants determined from plate's properties.

With the assumed displacement functions, the total potential energy of the stiffened plate can be calculated. The total potential energy is expressed in terms of the undetermined coefficients of the displacement functions and elements of the [*ABD*] matrices. Since a part of the approximate displacement function, $Y_n(y)$, was a piecewise function, calculation of the total potential energy had to be done section by section. To minimize the total potential energy with respect to the unknown coefficients A_{mn}, a set of linear equations is formed as follows

$$\frac{\partial \Pi}{\partial A_{mn}} = 0 \tag{3}$$

This set of equations may be written in form of a generalized eigenvalue problem as :

$$[A][C] - N_x[B][C] = 0 \tag{4}$$

[*A*] and [*B*] are square matrices whose elements are calculated based on the material properties and stacking sequence. [*C*] represents a column matrix containing the unknown eigenvector, i.e. the undetermined coefficients A_{mn}. N_x is the eigenvalue to be determined.

Eq. (4) was formed and solved using the computational program MAPLE [6]. The smallest eigenvalue is treated as the predicted buckling load and the corresponding eigenvector is treated as the buckling mode. The members of the eigenvector associated with the predicted buckling load were substituted into the displacement functions. Thus the out-of-plane displacement profile or buckling mode is obtained. The number of eigenvalue-eigenvector pairs equals the number of unknown coefficients contained within the column matrix [*C*]. Hence, the number of eigenvalue-eigenvector pairs is ultimately dictated by the number of terms used in the out-of-plane displacement field, Eq (1). If the number of terms (as dictated by values of *M* and *N*) used in Eq (1) is too low, then the magnitude of the predicted buckling load is overestimated, and/or the buckling mode is improperly predicted. Convergence studies of both load and mode were performed to ensure that solutions converged.

Experimental Study

Stiffened composite panels were mounted on a specially-designed loading frame and subjected to compressive-tensile biaxial loading as shown in Fig 3. The vertical compressive load was applied to a movable crosshead using a 10-ton hydraulic cylinder. The movable crosshead can be moves along four circular columns via linear bearings embedded within the crosshead. Transverse tensile loads were applied using two 5-ton pneumatic cylinders. Strain-gage based load cells were used to monitor the compressive and tensile loads. Tensile loading was controlled by adjusting the air pressure fed to the pneumatic cylinders. The pneumatic cylinders were connected to the specimen via notched aluminum plates. The aluminum plates were notched so that the effective stiffness of the aluminum plates in the vertical direction was negligible. Thus the composite specimen was not reinforced by the aluminum plate. Simply supported boundary condition along the compression edges was obtained by placing the top and bottom edges of the specimen into a slotted-steel rod as shown in Fig 4a. The middle part of the slotted rod was machined such that the stiffener can be placed in. These rods allowed the top and bottom edges of the specimen to rotate but restrict any out-of-plane displacement. Blade supports were used to enforce the simply supported boundary condition on both tension-loaded edges, as shown in Fig 4b. With these constraints, there was presumably no out-of-plane displacement on the contact lines between blade supports and the specimen. However, the panel was allowed to rotate in the out-of-plane direction.

Out-of-plane displacements induced during a test were monitored using shadow moiré [7]. A reference grating with a frequency of 3.3 lines/mm (83 lines/in) was used. The moiré fringes were recorded using a camcorder. The maximum out-of-plane displacements were also measured using mechanical dial gages with a measurement resolution of 0.025 mm (0.001 in). The mechanical measurement provided higher resolution than the optical measurement, but only displacement at a point was measured instead of the whole field displacement.

Specimens used in this study were fabricated using Toray T700S unidirectional graphite-epoxy prepreg. Ply properties are shown in Table 1. The stiffener strip was prepared by machining a thick flat plate into a long strip. These slender stiffeners were adhesively bonded to a thin rectangular flat plate, which formed the stiffened panel. The stiffened panel was then machined to a desired dimension. Specimens with three different stacking sequences and three different aspect ratios were tested. During the experiment, a constant and specified tension load was applied in the transverse direction. Then a compressive load in the vertical direction was increased until the fringe pattern from shadow moiré was clearly seen. Buckling modes were recorded. The points of maximum out-of-plane displacement were specified from the shadow moiré fringe. At this point, a relationship between a maximum out-of-plane displacement and an applied compressive load was determined by increasing the compressive load step by step and recording the corresponding out-of-plane displacement. Theoretically, a plot of compressive load against out-of-plane displacement shows two different slopes, those in the prebuckling region and postbuckling region [8,9]. Therefore, the buckling load can be experimentally specified at the point where slope of the load-displacement changes. Practically, experimental buckling point was located from the intersection of two straight lines drawn in those two regions. Measured buckling load and mode from the experiments were compared to the predictions obtained from the Ritz method.

Experimental Results

Three different combinations of skin and stiffener were considered. The stacking sequences considered are summarized in Table 2. Predicted and measured buckling loads of type-2 specimens are compared in Table 3 and are typical results. The skin in this case is $[0/90]_{2s}$ and the stiffener is $[0/90]_{6s}$. Due to space restrictions comparisons of the other two types of specimen are not presented in this paper.

Table 1. Mechanical properties of Toray T700S graphite epoxy

E_{11} (GPa)	E_{22} (Gpa)	G_{12} (GPa)	ν	Ply Thickness
113	7.88	3.73	0.3	0.15 mm

Table 2. Summary of the stacking sequences of the specimens

Type	Skin	Stiffener
1	$[0/90]_{2s}$	$[0]_{24}$
2	$[0/90]_{2s}$	$[0/90]_{6s}$
3	$[45/90/-45/0]_s$	$[\pm 45]_{6s}$

Table 3. Comparisons between predicted and measures buckling loads for Type-2 panels

Aspect Ratio	Tension, N_y, (kN/m)	Pred. Buckling Load, (kN)	Meas. Buckling Load, (kN)	% Error
1	0	16.5	17.3	-4.90
	8.78	19.8	21.1	-6.79
	17.56	21.3	23.5	-9.44
1.5	0	13.7	13.5	1.43
	8.78	16.9	15.1	11.7
	17.56	20.0	16.8	19.0
	26.33	22.5	25.6	-12.2
2	0	9.14	11.7	-22.3
	8.78	14.5	17.1	-15.4
	17.56	19.7	22.2	-11.8
	26.33	22.8	23.7	-4.06

The 3rd and 4th columns of Table 3. are the predicted and measured buckling loads, respectively. The percentage error in prediction was evaluated from

$$\%\text{Error} = \frac{N_{x(cri)}(\text{Pred}) - N_{x(cri)}(\text{Meas})}{N_{x(cri)}(\text{Meas})} \times 100\% \qquad (5)$$

Including the experiments shown in Table 3., a total of 30 experiments were conducted in this study. The percentage error in prediction ranged from –22.3% to +53.8% with an average of +8.62 % and a standard deviation of 21.1 %. Most of the data were in the range of ±25%. There were five experiments that had relatively high percentage of error. Qualitatively, measured buckling loads generally confirmed the predicted trend. For example, measured buckling loads increased as transverse tension increased, as predicted.

Some of the comparisons between measured and predicted buckling modes of type-2 specimen are shown in Table 4. Experiments on both uniaxial and biaxial loading of the specimen with aspect ratio of 1 yielded local buckling. Changing in number of mode from 2 to 3 was predicted by the Ritz method and was also observed in the experiment. The specimen with aspect ratio of 1.5 exhibited global buckling in the experiment with N_y = 17.56 kN/m. In contrast, during the experiment with N_y = 26.33 kN/m, the buckling mode shifted to mode 4 local buckling. This kind of shift in buckling mode demonstrated that increasing in transverse tension not only increases number of mode in local buckling, but also changes buckling mode from global to local. Similar behavior was obtained in the specimen with an aspect ratio of 2 which is not shown here. Generally, measured buckling modes were well predicted.

Although most of the experimental results generally confirmed the predictions, discrepancies between measurement and prediction were present in the experiment. Some experiments resulted in high percentage error in prediction of buckling loads. These experiment discrepancies are most likely due to imperfections of the specimens and test frame. Imperfections of the specimens include variations of thickness, variations of fiber angle, and preexisting curvatures. Imperfection of the test frame include inability to perfectly impose simply supported boundary condition, nonuniform loading, incapability to precisely apply compressive load on the mid-plane of the specimen, and reinforcement of aluminum loading plates to the specimens. These factors are always encountered during the experiment and are very difficult, if not impossible, to be eliminated. However these sources of error are also present in real engineering applications. Thus, it is reasonable to conclude that the measured buckling loads obtained in this study are credible and practical despite the discrepancies between measured and predicted buckling loads.

Conclusions

Buckling behaviors of rectangular stiffened composite panels were studied. Numerical predictions were obtained using the Ritz method. Total potential energy of a stiffened plate was calculated based on assumed displacement fields in form of proposed beam functions. The problem formulation ultimately led to an eigenvalue problem. The lowest eigenvalue and its corresponding eigenvector are the predicted buckling load and mode, respectively. Thirty tests were conducted on the rectangular stiffened panels. The measured buckling loads were relatively well predicted. The discrepancy between prediction and measurement in term of percentage error in prediction had an average value of +8.62%. The measured buckling loads increased with an increase in transverse tension, as predicted. The measured buckling modes were also well predicted. The mode number measured in instances of local buckling

compared well with predictions. Changes of buckling modes that were predicted due to a change in transverse tension were confirmed experimentally.

Acknowledgement

This research was developed under the supervision of Prof. Mark E.Tuttle of the University of Washington. The author is grateful for his guidance.

References

[1] Leissa, A.W., "A Review of Laminated Composite Plate Buckling," *App Mech Rev.*, 40, pp.575-91 (1987).

[2] Kapania, R.K. and Raciti,S., "Recent advances in analysis of laminated beams and plates, Part I: Shear effects and buckling," *AIAA Journal*, 27, pp.923-34 (1989).

[3] Whitney, J.M., Structural analysis of laminated anisotropic plates, Technomic Pub. Co., Lancaster, Pa., 1987.

[4] Reddy, J.N., Energy and variational methods in applied mechanics: with an introduction to the finite element method, Wiley, New York, 1984.

[5] Timoshenko, S., Young,D. H. and Weaver, Jr., W., Vibration problems in engineering, Wiley, New York, 1974.

[6] Maple V Release 5, Waterloo Maple Inc., 1997.

[7] Dally, J.W., and Riley, W.F., Experimental Stress Analysis, McGraw-Hill, New York, 1991.

[8] Leissa, A.W., "Advances in Vibration, Buckling and Postbuckling Studies on Composite Plates," Proceedings of the 1st International Conference on Composite Structures, Applied Science Publishers, London, pp.312-34 (1981).

[9] Tuttle, M., Singhatanadgid P., and Hinds, G., "Buckling of Composite Panels Subjected to Biaxial Loading", Experimental Mechanics, 39, pp. 191-201 (1999).

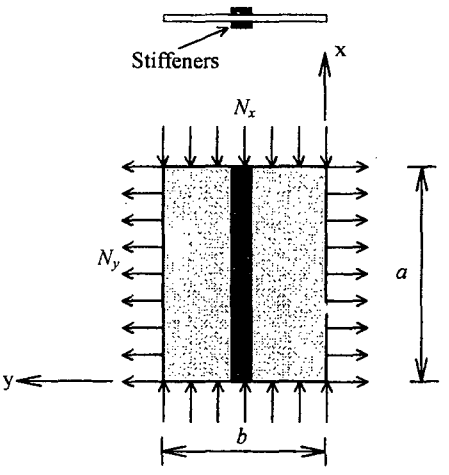

Fig 1. Position and shape of the stiffeners.

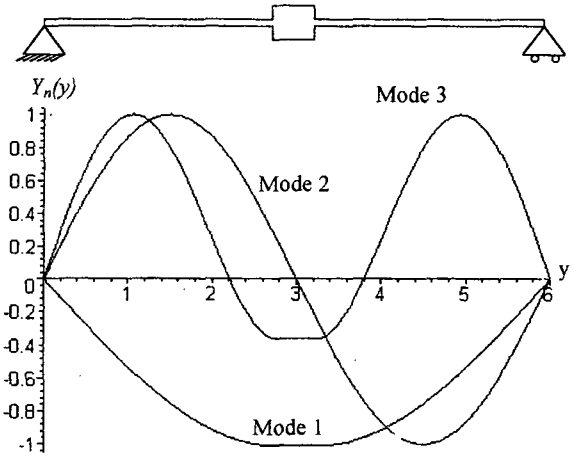

Fig 2. The first three mode shapes of a typical stepped beam

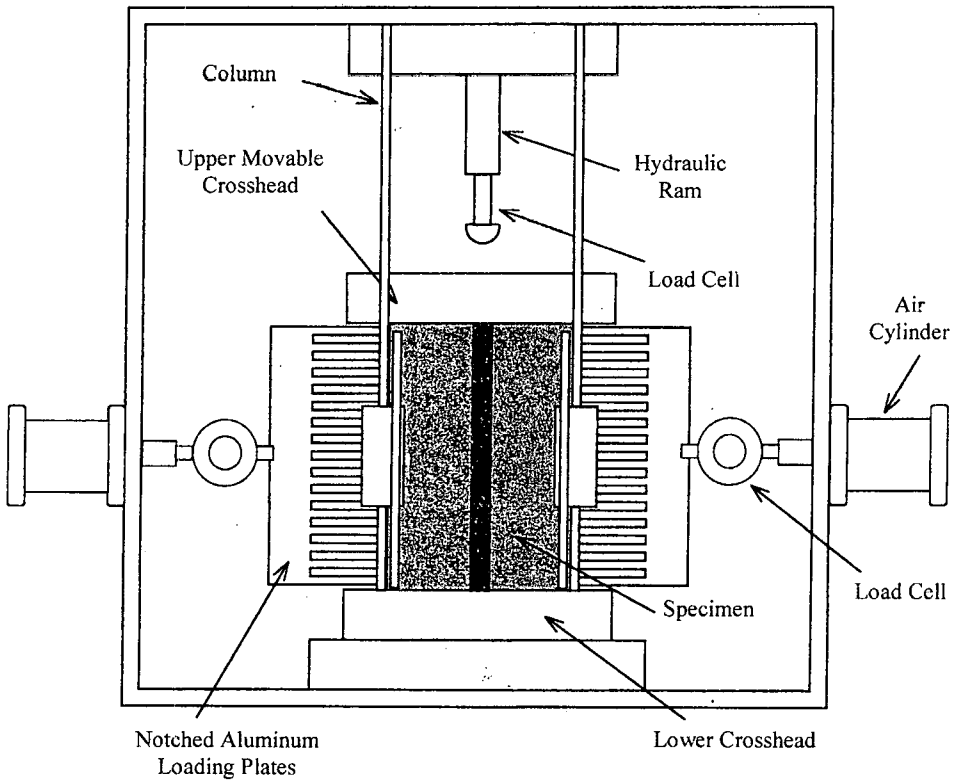

Fig 3. The schematic of tension-compression test frame

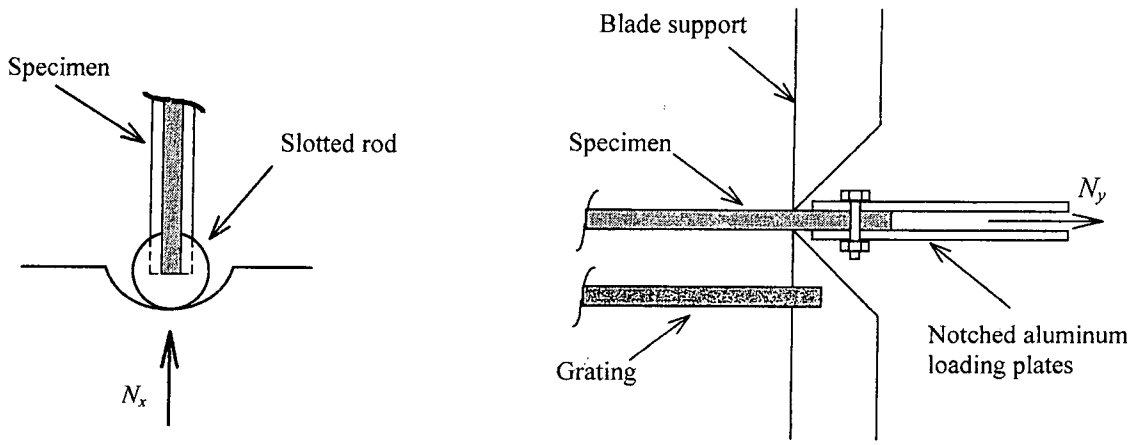

(a) Simple support along compression loaded edges (b). Simple support along tension loaded edges

Fig 4. Simply supported boundary conditions.

Table 4. Comparisons between predicted and measured buckling mode of Type-2 panel.

Aspect Ratio	1		1.5	
Tension N_y, (kN/m)	0	8.78	17.56	26.33
Prediction	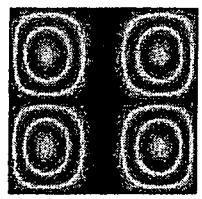	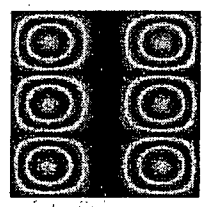	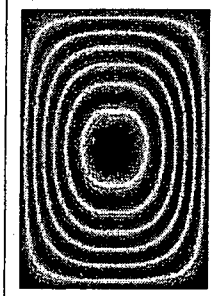	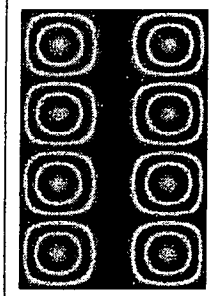
Measurement